VMAT inverse planning including DTI tractography fiber bundles as organs at risk: a feasibility study

Peroni M.[1,*], Patete P.[1], Ghielmetti F.[2,3],Casolino D.[1], Ongania E.[4], Casolino D.S.[4], Fariselli L.[3], Baroni G.[1,5]

[1]Department of Bioengineering, Politecnico di Milano, Milano, Italy
[2]Health Department and [3]Radiotherapy Unit Fondazione IRCCS Istituto Neurologico C. Besta, Milano, Italy
[4]Elekta AB, Stockholm, Sweden
[4]BioengineeringUnit, Centro Nazionale di Adroterapia Oncologica, Pavia, Italy

Abstract. The use of DTI tractography in radiosurgery and hypofractionated radiotherapy is still limited to visual inspection before planning to avoid tracts direct involvement. We propose to use the envelope of tractography fiber bundles as organs at risk, whose average dose shall be optimized during inverse planning. We show the benefit in terms of dose reduction, distribution homogeneity and target coverage in a feasibility study onto two glioma patients. The average dose at arcuate, corticospinal tract and corpus callosus was reduced respectively by 29%, 18% and 20% for patient 1 and 21%, 19% and 42% for patient 2. These promising preliminary results suggest that fiber bundles may be considered and preserved efficiently in radiation therapy treatment planning, allowing a potential increase of the total dose delivered to the target. The promising results prompt at integration also for benign and malignant small lesions treatment, where functional preservation is further critical.

Keywords: DTI, tractography, inverse planning, glioma

1 Introduction

Besides traditional anatomical Magnetic Resonance Imaging (MRI) sequences, functional MRI and Diffusion Tensor Imaging (DTI) offer a great potential to explore more complex functional and microscopic organization in the brain. DTI in particular allows the in-vivo visualization of the axonal organization of the white matter, exploiting the diffusion properties of water molecules [1-3]. Parameters like mean diffusivity and Fractional Anisotropy (FA) are commonly used as quantitative tools for differentiating the highly organized white matter from gray matter, as well as normal from pathological tissues [1,2] and for non-invasive pre-operative evaluation of tumor grade [4].
Based on the analysis of FA maps, water diffusion can be processed to reconstruct three-dimensional curves representing subcortical fiber tracts. This procedure, called

tractography, is based on mathematical algorithms that can be coarsely classified into deterministic and probabilistic approaches. Deterministic tractography methods rely on the assumption that, within a voxel, the orientation of the fibers is determined by the orientation of the main eigenvalue of the diffusion tensor [1,2,5]. This leads to anatomical reconstruction of the major white matter fibers, but its reliability is limited by image noise, distortions and fiber crossing [6]. To overcome deterministic approach limitations, probabilistic approaches have been proposed, in which a level of confidence is associated to each trajectory, starting from a set of seed points [1].
The largest field, where tractography is applied, is radiosurgery, in which a high radiation dose is delivered to the pathological tissue in one single treatment session. Koga et al [7] recently reported the outcomes of a prospective study on arteriovenous malformations in the brain in which DTI tractography was directly integrated into the Gamma-knife treatment planning workstation, with the long term goal of reducing radiation induced secondarisms and damages at cognitive areas, such as optic radiation, arcuate fasciculus and pyramidal and corticospinal tract. In [8-10], the authors estimated that the total dose tolerable by corticospinal tract is 2000cGy in a single Gamma-Knife radiosurgery session, while this value is reduced to 800cGy for the temporal fibers of arcuate fasciculus. The risk of steady sensory-motion decline is even higher if the selected treatment is radiotherapy and appears to be directly correlated with the field dimension. A preliminary study about the use of DTI in high-grade gliomas, conducted by Jena et al. [11], demonstrates the potentiality of using tractography in the personalization of treatment volumes according to tumor growth and infiltration grade. A major issue in all tractography works is represented by quantitative validation, since a real ground truth can be derived only from post-mortem histological slices. Anyway, some attempts have been made towards the objective evaluation of the tracts [12].
In the presented work, our goal is to use DTI deterministic tractography to define critical fiber bundles as organs at risk (OAR) in the inverse plan optimization of a Volumetric Modulated Arc Therapy (VMAT). We implemented a proof of concept study on two grade III glioma patients treated at the Fondazione IRCCS IstitutoNeurologico C. Besta (Milan, Italy) and demonstrated the feasibility of treatment arcs optimization in terms of total and mean dose at OARs, target coverage and homogeneity of dose distribution.

2 Materials and Methods

2.1 Dataset

Our retrospective study involves two grade III glioma patients (GS, m, 36 y, anaplastic oligoastrocytoma; SK, f, 38 y, anaplastic astrocytoma) who underwent anatomical MRI sequences (T1) for gross tumor volume (GTV) outline (with gadolinium contrast injection), DTI study for the surgical planning for tumor resection, and afterwards CT scan for the radiotherapy treatment planning and dose calculations. MRI sequences were acquired using a 1.5T SIEMENS Avanto scanner (SIEMENS HEALTHCARE, Erlangen, Germany). The MRI sequences were a morphological mprage T1 weighted

with resolution of 1x1x1mm, a DTI with 12 gradient directions EPI (echo Planar Imaging). DTI acquisition parameters were as follows: TE=92ms, TR=8.6s, voxel size =1x1x2 mm, 64 slices and b-value = 1000 s/mm^2. CT volumes were acquired using a Philips Brilliance scanner (Philips Healthcare, Eindhoven, the Netherlands) with 56 slices and a resolution of 0.9x0.9x3mm. Total planned dose for these patients was 5400 cGy, delivered in 200 cGy per fraction. For the purpose of this study, we simulated a VMAT hypofractionated treatment, for a total of 3000 cGy in 5 fractions.

2.2 Image pre-processing

For patient 1, DTI acquisition was performed 8 times, after which a mean volume was generated to enhance Signal to Noise Ratio (SNR). For patient 2, SNR was instead augmented by means of joint Rician filtering of each single diffusion direction.
Due to the different resolutions and reference frames of the acquired datasets, these were registered taking as reference the CT scan, as this is the core dataset for radiation therapy treatment planning and dose calculation. The registration of the DTI images on the CT was obtained by means of a three steps process. First of all the DTI gradients were registered on the *b=0* DTI volume (i.e. the images acquired with minimal diffusion weighting), to compensate for residual eddy currents and head motion. The obtained dataset was aligned to the corresponding anatomical MRI by means of an affine registration method based on normalized mutual information, using Slicer3D [13] routines. At the same time, we estimated the rigid transformation between anatomical MRI and CT, which we also applied to the aligned DTI volume.

2.3 Tractography algorithm

The corpus callosus, the corticospinal tract and the arcuate fasciculus ipsilateral to the neoplastic lesion were reconstructed using Slicer3D [13]. The chosen algorithm relies on a least-squares estimation of the diffusion tensor and on deterministic tracing of the fibers. The streamline path-integral deterministic algorithm at the basis of Slicer3D implementation was firstly described in [5] and solves the Frenet's equations using Runge-Kutta's numerical approximation.
To reconstruct the tracts of interest, we used a single ROI approach [14,15] based on existing anatomic knowledge about fiber bundles. This involved the help of expert neuro-radiologist and required the superimposition of T1 MRI and DTI tensor, whose dimensionality was reduced to a 3D volume condensing its information using a color map encoding for first eigenvector direction. The corpus callosus ROI was defined by contouring the fiber bundle on three sagittal slices into the hemisphere ipsilateral to the lesion. The corticospinal tract ROI seeding volumes were localized in three slices on the coronal view, where we contoured from the cerebral peduncle up to precentral gyrus. Arcuate fasciculus fibers originate in prefrontal and premotor gyri (part of the Broca's area) and project posteriorly to Wernicke's area, arching around the insula and putamen to run antero-inferiorly toward the temporal lobe. Arcuate ROI was individuated by successive approximation in axial and sagittal views at Wernicke's area level.

We used FA equal to 0.15 as stopping criteria for the estimation and 0.7°/mm as curvature escape condition, in an attempt of allowing a better estimation of fibers with large curvatures. We rejected fibers shorter than 10 mm and used voxel space for all calculations.

2.4 Post-processing and integration of tracts in the inverse treatment planning

The integration of reconstructed fibers in a radiation therapy treatment plan required the generation of appropriate 3D structures saved following the DICOM RT protocol. We designed and implemented a dedicated Qt- and VTK-based application, called fiberSlicer, to create the fiber bundles structure from the curves generated by Slicer3D and to extract their envelope contours, in order to create the required structures.
First of all, fiberSlicer approximates the single fiber with a tube of radius 0.75 times the CT pixel and central axis defined by the curve that identifies the fiber. The rendered bundle is cut according to each CT slice plane and the extracted object is triangulated using 2D Delaunay algorithm. The external contour on the cutting plane is than extracted and saved in DICOM RT format. The envelope contours may be saved separately or added to a previous DICOM RT file, to be easily imported by commercial workstations.
For the purpose of this preliminary study, we chose a commercial version of Elekta ERGO++(Elekta AB, Stockholm, Sweden), which supports Arc Modulation Optimization Algorithm (AMOA) inverse planning for VMAT treatments. With our approach, the fiber bundles can directly be assimilated to OARs and their minimum and maximum dose are used as constraints in AMOA fluence optimization. Besides fiber

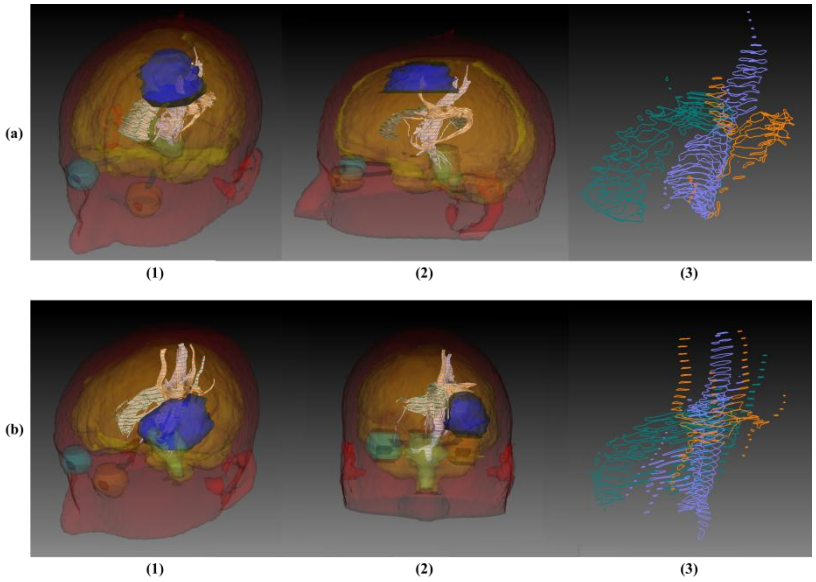

Fig.1. View of reconstructed fibers for patient 1 (a) and 2 (b) in fiberSlicer. Note the position of the fiber bundles with respect to the GTV (in solid blue). Panels (a.3) and (b.3) show the envelope of the reconstructed fascicles, which are used as OARs for dose inverse planning.

bundles, the attending physician contoured also other OARs, including brain, eyes, optical nerves, crystalline lenses, optical chiasm, and brainstem. As these structures were reasonably distant from the target, in this preliminary study, we did not introduce constraints on these OARs.
To quantify the potential benefits of including DTI tractography in radiation therapy planning, we performed an initial plan consisting of 94 beams divided into 5 arcs without any constraint on the fibers and subsequently an inverse planning including fiber bundles as OARs. The plans were compared in terms of Dose Volume Histogram (DVH) of both target and OARs, as well as in terms of cumulated dose at the fibers. Dose matrices calculations were performed on a 3mm grid for patient 1 and 2mm grid for patient 2.

2.5 Optimization procedure

Under the advice of the attending physicists, we decided to ignore corpus callosus in VMAT arcs optimization, under the hypothesis this structure being less critical. For both patients, the maximum dose at corticospinal tract and arcuate fasciculus was set at 800 cGy, applied to 70% and 60% volumes respectively (i.e. the constraint is applied to the volume fraction, while there is no control on the remaining part of the OAR structure). The penalty for the violation of these constraints was 10^4. For the chosen hypofractionated treatment, minimum and maximum dose constraints on the Gross Tumor Volume (GTV) were set at 95% (2850cGy) and 105%(3150cGy) of the total dose delivered. The penalties for these constraints were set respectively to 10^4 and $1.5 \cdot 10^4$, and the condition was restricted to the 98% of the GTV volume.

3 Results

3.1 Fiber bundles reconstruction and slicing

From the selected ROIs we were able to reconstruct anatomically reliable tracts.

Table1. Minimum, Maximum and Average Cumulative Dose before (rVMAT) and after (oVMAT) AMOA inverse planning for Gross Tumor Volume (GTV), Corpus Callosum (CC), Arcuate Fasciculus (AF) and CorticoSpinal Tract (CST).

	Organ	Minimum [cGy]		Maximum [cGy]		Average [cGy]	
	At Risk	rVMAT	oVMAT	rVMAT	oVMAT	rVMAT	oVMAT
Patient 1	**GTV**	2400	2370	3060	3030	2924	2922
	CC	240	210	1200	870	502	395
	AF	300	180	2970	3000	1014	720
	CST	090	060	2910	2880	1000	819
Patient 2	**GTV**	2010	1680	3060	3120	2913	2900
	CC	330	180	2880	2880	906	527
	AF	120	90	2970	2970	1551	1223
	CST	120	120	2970	2880	1480	1203

Figure 1 shows the obtained bundles for patient 1 and 2 in panels a and b respectively. In patient 1, corticospinal tract was entering directly into lesion volume and, as such, this tract is very likely to be compromised by radiation. Corpus callosus and arcuate fasciculus are also located in the immediate proximity to the tumor. Patient 2 tracts were reconstructed less accurately (Figure 1b). In particular, arcuate fasciculus integrity was compromised by the massive lesion and therefore lost the typical arch. In figure 1 (Panels a.3 and b.3), note also the color envelope superimposed onto the tube dilation of the fiber axes and that the different fiber bundles were kept separated in the attempt of differentiating tracts involvement in the treatment.

3.2 Dosimetric evaluation

DVHs of cumulative dose obtained from VMAT without any dose optimization (rVMAT) are presented in Figure 2a and 2c for patient 1 and 2 respectively. In panels b and d, we show the distribution obtained after inverse planning (oVMAT) with constraints on GTV, arcuate and corticospinal tracts only. We note that the coverage of the GTV is maintained also in b and d, whilst a better sparing of both arcuate fasciculus and corticospinal tract is possible. Despite not setting any constraint on corpus callosus, its final dose distribution is improved after optimization.
Cumulative average, maximum and minimum dose at GTV, corpus callosus, arcuate fasciculus and corticospinal tract is also reported in Table 1. For patient 2, the optimized distribution loses in conformity in particular at lower dose grades, while for patient 1 the 95% isodose distribution is very similar to pre-inverse planning one.
We were able to further optimize patient 1 distribution, changing dose constraint on the fiber bundles. The new maximum dose was chosen as the one at 50% volume after first optimization, but it was applied to the volume used in the first optimization run (600 cGy on 60% of the volume and 500 cGy on 70% of the volume for arcuate and corticospinal tracts respectively). Average dose dropped in this case to 571 cGy, 716 cGy and 264 cGy for arcuate, corticospinal and corpus callosus respectively, while GTV mean dose remains at 2914 cGy. The GTV distribution was still homogeneous enough to consider this further optimization suitable for the clinic.

4 Discussion and conclusion

In this feasibility study, we propose to directly incorporate DTI tractography reconstructed fiber bundles into AMOA inverse planning for VMAT hypofractionated treatment. We performed tractography of corticospinal tract, arcuate fasciculus and corpus callosum in the hemisphere ipsilateral to grade III glioma lesion. Tractography quality was visually inspected by the attending physicians and physicists, but more quantitative validation shall be performed in future studies. The error induced by tumor proximity to the tracts as well as by the edema surrounding the neoplastic lesion reflected on tractography quality, as previously shown in terms of FA values by [16]. In particular, patient 2 lesion severely dislocated and interrupted the arcuate fasciculus in the medial region.

Despite the need for further refinement and quantitative validation of fiber bundles, we were able to integrate all tracts into the treatment planning after calculating their envelope with an *adhoc* developed software called fiberSlicer. The smoothness and continuity of the contours was guaranteed by Delaunay triangulation of the sliced surfaces. Therefore, the treatment planning system handled the fiber bundles exactly as all other manually contoured structures.

Considering the fiber bundles in the plan optimization, we were able to strongly reduce the dose delivered to the corticospinal and arcuate tracts, while the optimized target DVH remain mostly unchanged. On the other side, the non-significant difference in the maximum total dose at fibers is due to the fact that the fiber bundles projected inside the GTV, but the shape of their DVH curves after optimization tends to be similar to the typical OAR ones. Further forcing of the maximum dose constraint might prevent optimization convergence and/or escalate dose distribution inhomogeneity. The average dose at arcuate, corticospinal tract and corpus callosus was reduced respectively by 29%, 18% and 20% for patient 1 and 21%, 19% and 42% for patient 2, confirming that this method has the potential to be applicable for planning, enhancing fiber bundles sparing and possibly enhancing functionality preservation.

Future work will be dedicated to enlarge patient database and adding specific dose constraints for all the organs at risk and running a more complex inverse planning. In addition, the promising results underlined by our feasibility study will be extended to high precision treatments (e.g. Cyberknife) of small lesions (benign and malignant) in

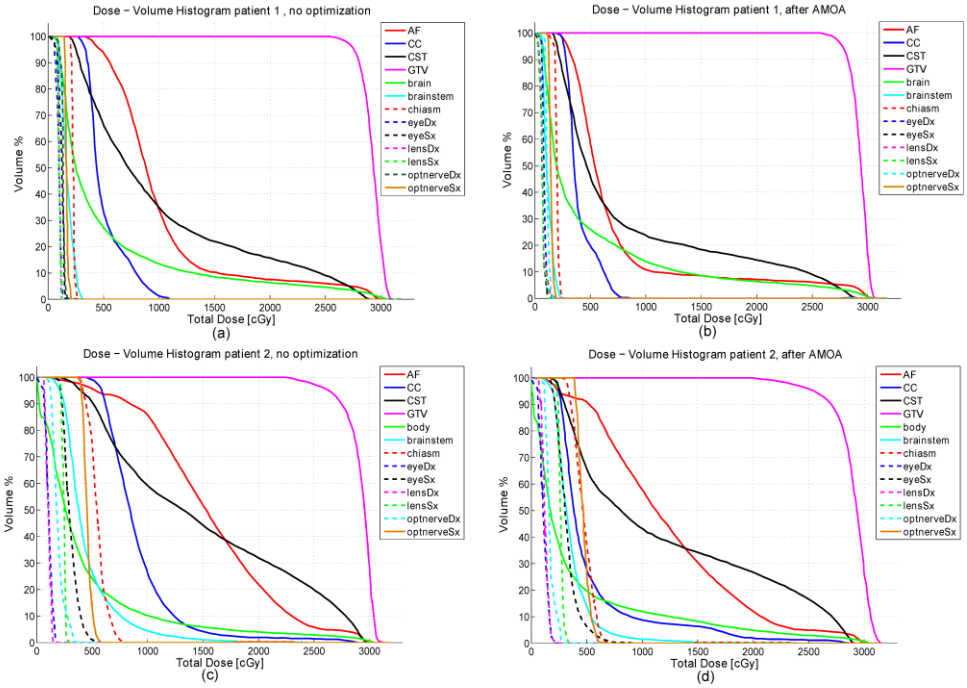

Fig.2. Dose Volume Histogram (DVH) comparison for patient 1 (a,b) and 2 (c,d). Panels a and c show DVHs of both GTV and OARs before inverse planning optimization, while b and d report the results after optimization. Note that in b and d dose of fiber bundles is lower than in the non-optimized version, despite the constant GTV coverage.

critical functional areas.

5 Bibliography

1. Yamada K., Sakai K., Akazawa K., Yuen S., Nishimura T. MR tractography: a review of its clinical applications. Magnetic resonance in medical sciences MRMS an official journal of Japan Society of Magnetic Resonance in Medicine 8, 165-74 (2009).
2. Masutani Y., Aoki S., Abe O., Hayashi N., Otomo K., MR diffusion tensor imaging: recent advance and new techniques for diffusion tensor visualization, European Journal of Radiology, 46(1): 53-66, (2003)
3. Le Bihan D, Mangin JF, Poupon C, Clark CA, Pappata S, Molko N, Chabriat H., Diffusion tensor imaging: concepts and applications., J Magn Reson Imaging., Apr;13(4):534-46 (2001)
4. Inoue T., Ogasawara K., Beppu T., Ogawa A., Kabasawa H., Diffusion tensor imaging for preoperative evaluation of tumor grade in gliomas, Clinical Neurology and Neurosurgery, Apr; 107(3): 174-180 (2005).
5. Basser PJ, Pajevic S, Pierpaoli C, Duda J, Aldroubi A., In vivo fiber tractography using DT-MRI data., Magn Reson Med. Oct;44(4):625-32 (2000).
6. Chung HW, Chou MC, Chen CY., Principles and limitations of computational algorithms in clinical diffusion tensor MR tractography.,AJNR Am J Neuroradiol., Jan;32(1):3-13. (2011).
7. Koga, T. et al. Outcomes of diffusion tensor tractography-integrated stereotactic radiosurgery. International Journal of Radiation Oncology, Biology, Physics 82, 799-802 (2012).
8. Maruyama K, Kamada K, Shin M, Itoh D, Aoki S, Masutani Y, Tago M, Kirino T., Integration of three-dimensional corticospinal tractography into treatment planning for gamma knife surgery., J Neurosurg. Apr;102(4):673-7. (2005)
9. Maruyama K, Koga T, Kamada K, Ota T, Itoh D, Ino K, Igaki H, Aoki S, Masutani Y, Shin M, Saito N., Arcuate fasciculus tractography integrated into Gamma Knife surgery., J Neurosurg. Sep;111(3):520-6.(2009)
10. Maruyama K, Shin M, Tago M, Kurita H, Kawamoto S, Morita A, Kirino T., Gamma knife surgery for arteriovenous malformations involving the corpus callosum.J Neurosurg. Jan;102 Suppl:49-52. (2005)
11. Jena R, Price SJ, Baker C, Jefferies SJ, Pickard JD, Gillard JH, Burnet NG., Diffusion tensor imaging: possible implications for radiotherapy treatment planning of patients with high-grade glioma., Clin Oncol , Dec;17(8):581-90.(2005)
12. Wang JY, Abdi H, Bakhadirov K, Diaz-Arrastia R, Devous MD Sr., A comprehensive reliability assessment of quantitative diffusion tensor tractography.Neuroimage. Apr 2;60(2):1127-38 (2012).
13. Pieper S., Lorensen B., Schroeder W., Kikinis R., The NA-MIC Kit: ITK, VTK, Pipelines, Grids and 3D Slicer as an Open Platform for the Medical Image Computing Community., Proceedings of the 3rd IEEE International Symposium on Biomedical Imaging: From Nano to Macro 2006; 1:698-701 (2006).
14. Wakana S, Jiang H, Nagae-Poetscher LM, van Zijl PC, Mori S., Fiber tract-based atlas of human white matter anatomy., Radiology. Jan;230(1):77-87 (2002).
15. Catani M, Howard RJ, Pajevic S, Jones DK., Virtual in vivo interactive dissection of white matter fasciculi in the human brain., Neuroimage. Sep;17(1):77-94 (2002).
16. Yen PS, Teo BT, Chiu CH, Chen SC, Chiu TL, Su CF., White Matter tract involvement in brain tumors: a diffusion tensor imaging analysis., Surg Neurol. Nov;72(5):464-9; (2009).